HHS Public Access

Author manuscript

Nature. Author manuscript; available in PMC 2016 January 16.

Published in final edited form as:

Nature. 2015 July 16; 523(7560): 347–351. doi:10.1038/nature14406.

Conversion of abiraterone to D4A drives antitumor activity in prostate cancer

Zhenfei Li[1], **Andrew Bishop**[1], **Mohammad Alyamani**[1], **Jorge A. Garcia**[2,3], **Robert Dreicer**[2,3], **Dustin Bunch**[4], **Jiayan Liu**[5], **Sunil K. Upadhyay**[5], **Richard J. Auchus**[5], and **Nima Sharifi**[1,2,3]

[1]Department of Cancer Biology, Lerner Research Institute, Cleveland Clinic, Cleveland, OH

[2]Department of Hematology and Oncology, Taussig Cancer Institute, Cleveland Clinic, Cleveland, OH

[3]Department of Urology, Glickman Urological and Kidney Institute, Cleveland Clinic, Cleveland, OH

[4]Department of Laboratory Medicine, Pathology and Laboratory Medicine Institute, Cleveland Clinic, Cleveland, OH

[5]Division of Endocrinology and Metabolism, Department of Internal Medicine, University of Michigan Medical School, Ann Arbor, MI

Summary

Prostate cancer resistance to castration occurs because tumors acquire the metabolic capability of converting precursor steroids to 5α-dihydrotestosterone (DHT), promoting signaling by the androgen receptor (AR) and the development of castration-resistant prostate cancer (CRPC)[1–3]. Essential for resistance, DHT synthesis from adrenal precursor steroids or possibly from *de novo* synthesis from cholesterol commonly require enzymatic reactions by 3β-hydroxysteroid dehydrogenase (3βHSD), steroid-5α-reductase (SRD5A) and 17β-hydroxysteroid dehydrogenase (17βHSD) isoenzymes[4,5]. Abiraterone, a steroidal 17α-hydroxylase/17,20-lyase (CYP17A1) inhibitor, blocks this synthetic process and prolongs survival[6,7]. We hypothesized that abiraterone is converted by an enzyme to the more active Δ^4-abiraterone (D4A) that blocks multiple steroidogenic enzymes and antagonizes the androgen receptor (AR), providing an additional explanation for abiraterone's clinical activity. Here we show that abiraterone is converted to D4A in mice and patients with prostate cancer. D4A inhibits CYP17A1, 3βHSD and SRD5A, which are required for DHT synthesis. Furthermore, competitive AR antagonism by D4A is comparable to the potent antagonist, enzalutamide. D4A also has more potent antitumor activity against xenograft tumors than abiraterone. Our findings suggest an additional explanation – conversion to

Correspondence: Nima Sharifi, Phone: 216 445-9750, FAX: 216 445-6269, sharifn@ccf.org.

Author Contributions

Z.L. performed gene expression, metabolism, ChIP and mouse xenograft studies. A.B., M.A. and D.B. performed mass spectrometry studies. J.A.G. and R.D. participated in clinical studies. J.L. and S.K.U. performed enzymology studies, and S.K.U. also performed chemical syntheses. Z.L., R.J.A and N.S. designed the studies and wrote the manuscript. All authors discussed the results and commented on the manuscript.

a more active agent – for abiraterone's survival extension. We propose that direct treatment with D4A would be more clinically effective than abiraterone treatment.

The central role and critical requirement for androgen metabolism and AR in CRPC are demonstrated by the clinical benefit and overall survival benefit conferred by abiraterone (Abi)[6,7], which blocks CYP17A1, an enzyme required for androgen synthesis, and enzalutamide, which potently and competitively blocks the AR[8,9]. Abi (administered in its acetate form for bioavailability) is a steroidal compound and is therefore potentially subject to conversion by steroid-metabolizing enzymes. We hypothesized the Δ^5, 3β-hydroxyl-structure of Abi, which is also present in the natural steroid substrates dehydroepiandrosterone (DHEA) and Δ^5-androstenediol (A5diol), makes it susceptible to one enzyme conversion by 3βHSD isoenzymes to its Δ^4, 3-keto congener (Δ^4-abiraterone or D4A), which would make the steroid A and B rings identical to testosterone (T), enabling inhibitory interactions with AR and additional steroidogenic enzymes, including SRD5A, which are required for DHT synthesis (Fig. 1a). Such a conversion in peripheral tissues would allow D4A to engage with multiple targets to potentiate its effects on the androgen pathway, providing an alternative explanation for the clinical efficacy of Abi therapy and thus the possibility that direct treatment might be more efficacious.

We found that D4A is detectable in the sera of mice administered Abi acetate (Fig. 1b), as well as in sera from patients with CRPC who were undergoing treatment with Abi acetate (Fig. 1c, 1d and Extended Data Fig. 1). In the LAPC4 prostate cancer cell line, which usually has low 3βHSD activity[3], conversion of Abi to D4A is detectable only if 3βHSD is overexpressed (Fig. 1e and Extended Data Fig. 2a–b). Other tissues such as the mouse adrenal (but not mouse prostate) that have robust endogenous 3βHSD enzymatic activity also convert Abi to D4A (Extended Data Fig. 2c). These results suggest that D4A is a major metabolite of Abi, requires 3βHSD for conversion, and may confer effects on the tumor that are indirectly due to Abi.

D4A may impinge on multiple steps in the androgen pathway, including CYP17A1, 3βHSD, SRD5A and direct interaction with AR (Fig. 2a). Although augmented Abi drug exposure may block 3βHSD, normal dosing probably does not[10]. On the other hand, D4A is approximately 10-fold more potent than Abi at blocking the conversion of [^{3}H]-DHEA by 3βHSD to Δ^4-androstenedione (AD) in LNCaP and VCaP cells, as assessed by thin layer chromatography (TLC; Extended Data Fig. 3a) and high performance liquid chromatography (HPLC; Fig. 2b, Extended Data Fig. 3b). D4A inhibits both human isoenzymes, 3βHSD1 and 3βHSD2, with mixed inhibition kinetics (Fig. 2c). CYP17A1 inhibition is the major direct mechanism of action for Abi[11]. Structural studies of modified steroidal azoles suggest that the A-ring conformation of D4A does not significantly perturb binding to CYP17A1[12]. D4A and Abi similarly block conversion of [^{3}H]-pregnenolone by CYP17A1 to DHEA (% conversion to DHEA after 3 h incubation for vehicle, 1 nM D4A and 1 nM Abi is 70.1%, 4.2% and 2.6%, respectively) by HPLC in intact 293 cells expressing CYP17A1 (Fig. 2d). The Δ^4, 3-keto-structure of D4A is identical to physiologic SRD5A substrates, such as T and AD (Fig. 1a)[13]. To determine the effect of D4A on endogenously expressed SRD5A, LAPC4 cells, which exhibit robust SRD5A enzymatic

activity[13] were treated with D4A, Abi or enzalutamide, and cultured in the presence of [^{3}H]-AD (the preferred natural substrate of SRD5A1[13]). D4A (10μM) nearly completely blocks conversion from AD to 5α-androstanedione and other 5α-reduced androgens, whereas Abi and enzalutamide have no detectable effect even at a concentration of 100 μM (Fig. 2e).

Abi has been reported to have modest affinity for AR, particularly in the presence of mutations in the ligand-binding domain (LBD)[14]. Conversion of Abi by 3βHSD to D4A would provide a 3-keto structure, which is shared with both T and DHT, steroids with the highest affinity for AR (Fig. 1a). To determine how conversion from Abi to the 3-keto structure of D4A affects drug affinity for AR, we performed a competition assay. The affinity of D4A for mutant (expressed in LNCaP, IC_{50} = 5.3 nM) and wild-type (expressed in LAPC4, IC_{50} = 7.9 nM) AR is greater than that of Abi (IC_{50} = 418 and > 500 nM, respectively), comparable to or slightly greater than that of enzalutamide (IC_{50} = 24 and 23 nM, respectively, Fig. 3a–b), and clearly greater than bicalutamide, which was the most potent competitive nonsteroidal AR antagonist prior to the introduction of enzalutamide (Extended Data Fig. 4a–b). The affinity of D4A for the AR LBD translates to inhibition of DHT-induced AR chromatin occupancy on the *PSA*, *TMPRSS2* and *FKBP5* regulatory elements on chromatin, which is superior to Abi (Extended Data Fig. 4c) and somewhat lower than enzalutamide (Fig. 3c). The incongruity between AR affinity and effects on chromatin occupancy for D4A and enzalutamide is consistent with combined AR antagonism and chromatin binding in an inactive complex as previously reported for some AR antagonists[15].

We next examined the cumulative results of the effects of D4A on androgen-responsive gene expression. Compared to Abi, D4A clearly better suppresses *PSA*, *TMPRSS2* and *FKBP5* expression induced by DHT, DHEA and R1881 in LNCAP, LAPC4 and C4-2 cell lines (Fig. 3d and Extended Data Fig. 5a and 5c). D4A inhibits AR target gene expression in a dose-dependent manner (Extended Data Fig. 5b and 5d). Comparisons of D4A to enzalutamide on DHT-induced endogenous *PSA* expression demonstrate that D4A is equivalent to enzalutamide against mutant and wild-type AR (Fig. 3e–f and Extended Data Fig. 5c–d). Downstream of androgen-responsive gene expression, effects of D4A and enzalutamide on DHT-stimulated cell growth are equivalent (Fig. 3g), both of which are more potent than Abi.

To determine whether the observed effects of D4A on inhibition of steroid synthesis demonstrated in tissue culture also occur in tumors, effects in two prostate cancer xenograft models with robust 3βHSD enzymatic activity[3] were assessed. Subcutaneous mouse xenograft tumors of VCaP and LNCaP cells, which both harbor a mutant gene encoding a missense in 3βHSD1 that effectively increases enzyme activity[3], were grown in male NSG mice. Fresh tumors were harvested, minced and incubated with [^{3}H]-DHEA plus Abi or D4A (0.1–10 μM). Similar to effects shown in Fig. 2, D4A is 10-fold more potent than Abi in blocking conversion from DHEA by 3βHSD to AD in LNCaP (Fig. 4a) and VCaP xenografts (Fig. 4b). For example, 0.1 μM D4A is equivalent to 1 μM Abi for blocking AD accumulation at 48 hr in both LNCaP and VCaP xenografts. To test whether the combined effects of D4A on inhibition of steroid synthesis and direct blockade of AR lead to augmented anti-tumor activity compared with Abi, VCaP xenografts were grown

subcutaneously in orchiectomized mice with DHEA pellet implantation (to mimic human adrenal physiology; Fig. 4c). Time from initiation of treatment with D4A, Abi acetate or vehicle, to tumor progression (> 20% increase in tumor volume) was assessed by generating Kaplan-Meier survival curves and comparing treatment groups with the log-rank test. Progression was significantly delayed in the D4A group compared to the Abi acetate group ($P = 0.011$). Fold-change in tumor volume is shown for each treatment group in Extended Data Fig. 6. We also compared xenograft growth using the same method with the C4-2 cell line model. D4A treatment increased progression-free survival compared to Abi acetate and enzalutamide (Fig. 4d). In serum collected from D4A treated mice at the end of the xenograft study there was no detectable increase in deoxycorticosterone, which is the mineralocorticoid that is most highly elevated in patients treated with Abi acetate, causing hypertension and hyperkalemia (Extended Data Fig. 7)[6,16]. Fig. 4e depicts the multiple points in the androgen pathway at which conversion of Abi by 3βHSD to D4A in patients impinges on AR signaling and prostate cancer progression, and the relative potencies of D4A, Abi and enzalutamide.

The next-generation hormonal therapies, Abi and enzalutamide, each have a single predominant target (CYP17A1 and AR, respectively). These drugs have clinically validated that androgen synthesis and AR stimulation are both essential components required to spur the development and progression of CRPC. After oral administration, Abi acetate is hydrolyzed and thereby converted to Abi, which is thought to be the major active agent by way of blocking CYP17A1. The major recognized metabolites of Abi result from hepatic CYP3A4 and SULT2A1 processing, forming the N-oxide of Abi and Abi sulfate, respectively. Neither of these modifications affects the Δ^5, 3β-hydroxyl-structure of the steroid backbone. In contrast, conversion to D4A modifies the steroidal structure to one that more robustly engages with AR, SRD5A and 3βHSD, thereby blocking androgen signaling at all these steps, while retaining CYP17A1 inhibition. The clinical significance of conversion of Abi to D4A and effects on individual components of the androgen pathway in patients must be viewed in light of pharmacokinetic studies which show a C_{max} of approximately 1 μM and also wide interpatient variability[16]. Furthermore, our findings suggest that D4A also has much more potent anti-tumor activity against CRPC when directly compared to Abi.

The potential clinical utility of treating CRPC patients directly with D4A is dependent on the underlying mechanisms of resistance to Abi, which have not been fully elucidated and the clinical settings in which the benefit from Abi is exhausted. The evidence suggests that sustained AR signaling characterizes at least a subset of Abi resistance cases. For example, increased AR copy number in CRPC is associated with absence of clinical response to Abi[17] and increased AR protein expression appears to occur upon the development of acquired clinical resistance to Abi[18]. Although Abi is a potent CYP17A1 inhibitor, studies of urinary steroid metabolites in patients demonstrate that androgen synthesis inhibition is incomplete, raising the possibility of sustained steroidogenesis as a mechanism of resistance[5,19]. Clinically, the combination of CYP17A1 inhibition and a potent AR antagonist appears to confer more potent androgen signaling inhibition in patients with CRPC[20].

Circulating concentrations of D4A in patients treated with Abi acetate appear to be quite variable. In contrast to hepatic Abi metabolites, it is probable that conversion of Abi to D4A in peripheral tissues leads to D4A concentrations that are higher in peripheral tissues (such as CRPC) than are present in serum. The effects of D4A on androgen signaling in CRPC, in particular distal steps in DHT synthesis and activity as an AR antagonist, may therefore be underestimated based on serum concentrations alone. Nonetheless, D4A levels in peripheral tissues and the precise contribution of D4A to the clinical activity of Abi have yet to be determined.

Finally, our results raise the possibility that there may be a previously unappreciated class effect of steroidal versus nonsteroidal CYP17A1 inhibitors. In contrast to Abi acetate, TAK-700, a nonsteroidal CYP17A1 inhibitor, failed to prolong survival in metastatic CRPC[21]. It is possible that the absence of active downstream steroidal metabolites may have contributed to these findings. This issue should be considered as other steroidal and nonsteroidal CYP17A1 inhibitors undergo further clinical investigation.

In conclusion, we have identified a novel Abi metabolite that is present in patients with CRPC treated with Abi acetate and has more potent anti-tumor activity than the parent drug. Conversion to D4A may be responsible for some of the clinical activity observed with the use of Abi. We suggest that treatment with D4A is likely to result in a greater clinical benefit than Abi.

METHODS

Cell lines

LNCaP and VCaP cells were purchased from the American Type Culture Collection (Manassas, VA) and maintained in RPMI-1640 with 10% FBS. LAPC4 cells were kindly provided by Dr. Charles Sawyers (Memorial Sloan Kettering Cancer Center, New York, NY) and grown in Iscove's Modified Dulbecco's Medium with 10% FBS. C4-2 cells were kindly provided by Dr. Leland Chung (Cedars-Sinai Medical Center, Los Angeles, CA) and maintained in RPMI-1640 with 10% FBS. All experiments done with LNCaP and VCaP were done in plates coated with poly-DL-ornithine (Sigma-Aldrich, St. Louis, MO). A 293 cell line stably expressing human CYP17A1 was generated by transfection with plasmid pcDNA3-CYP17 (a generous gift of Dr. Walter Miller, University of California, San Francisco) and selection with G418 as described[22]. Cell lines was authenticated by DDC Medical (Fairfield, OH) and determined to be negative mycoplasma free with primers 5′-ACACCATGGGAGCTGGTAAT-3′ and 5′-GTTCATCGACTTTCAGACCCAAGGCAT-3′.

Chemicals

Abi acetate was purchased from Medkoo Biosciences (Chapel Hill, NC). Abi and D4A were synthesized as described previously[10]. Enzalutamide was obtained from Medivation (San Francisco, CA).

Steroid metabolism

Cell Line Metabolism: Cells were seeded and incubated in 12-well plates with 0.2 million cells/well for ~24 h and then incubated with a mixture of radioactive ([^{3}H]-labeled) and non-radioactive androgens (final concentration, 100 nM; ~1,000,000 cpm/well; PerkinElmer, Waltham, MA) at 37°C. Aliquots of medium were collected at the indicated times. Collected medium was treated with 1,000 units of β-glucuronidase (Helix pomatia; Sigma-Aldrich) at 65°C for 2 h, extracted with 860 μL ethyl acetate:isooctane (1:1), and concentrated under nitrogen gas. Xenograft Metabolism: 10^7 LNCaP or VCaP cells were injected subcutaneously with Matrigel into surgically orchiectomized NSG mice that were implanted with 5 mg 90-day sustained-release DHEA pellets (Innovative Research of American, Sarasota, FL). Xenografts were harvested when they reached 1000 mm^3, minced, and cultured in DMEM with 10% FBS at 37°C with mixture of radioactive ([^{3}H]-labeled) and non-radioactive androgens, or Abi, when they reached 1000 mm^3. Each xenograft was analyzed in triplicate in at least three independent experiments. Aliquots of medium were collected at the indicated times. Collected medium was treated with 1,000 units of β-glucuronidase at 65°C for 2 h, extracted with 860 μL ethyl acetate:isooctane (1:1), and concentrated under nitrogen gas.

High-performance liquid chromatography (HPLC) analysis was performed on a Waters 717 Plus HPLC or an Agilent 1260 HPLC. Dried samples were reconstituted in 50% methanol and injected into the HPLC. Steroids and drug metabolites were separated on Kinetex 100 × 2.1 mm, 2.6 μm particle size C_{18} reverse-phase column (Phenomenex, Torrance, CA) using a methanol/water gradient at 30°C. The column effluent was analyzed using a dual-wavelength UV-visible detector set at 254 nm or β-RAM model 3 in-line radioactivity detector (IN/US Systems, Inc.) using Liquiscint scintillation cocktail (National Diagnostics, Atlanta, GA). Alternatively, dried samples were applied to plastic-backed silica gel plates and separated by thin-layer chromatography (TLC) using a mobile phase of 3:1 chloroform:ethyl acetate, followed by exposure of the plates to a phosphorimager screen and quantitated with a Storm model 860 phosphorimager (Applied Biosystems, Foster City, CA). All HPLC and TLC studies were conducted in triplicate and repeated at least 3 times in independent experiments. Results are shown as mean ± SD.

Gene expression

Cells were starved with phenol red-free and serum free-medium for at least 48 h and treated with the indicated drugs and/or androgens. RNA was extracted with a GenElute Mammalian Total RNA miniprep kit (Sigma-Aldrich). cDNA was synthesized from 1 μg RNA in a reverse transcription reaction using the iScript cDNA Synthesis Kit (Bio-Rad, Hercules, CA). Quantitative PCR (qPCR) analysis was conducted in triplicate with primers for *PSA*, *TMPRSS2*, *FKBP5*, and *RPLPO* described previously[3], with an ABI 7500 Real-Time PCR machine (Applied Biosystems) using iTaq Fast SYBR Green Supermix with ROX (Bio-Rad) in 96-well plates at a final reaction volume of 20 μL. Accurate quantitation of each mRNA was achieved by normalizing the sample values to *RPLPO* and to vehicle-treated cells.

ChIP assay

LNCaP cells were serum-starved for at least 48 h and treated with indicated drugs and DHT for 3 h. A ChIP assay was performed with an anti-AR antibody (Santa Cruz, sc-816) as described previously[23]. All of the precipitated DNA samples were quantified by qPCR and normalized to input DNA. All ChIP experiments were performed at least three times. Primers used for ChIP experiments are from experiments previously described[24]. Primer sequences are as follows: *PSA*: 5′-TGGGACAACTTGCAAACCTG-3′ and 5′-CCAGAGTAGGTCTGTTTTCAATCCA-3′; *FKBP5*: 5′-CCCCCTATTTTAATCGGAGTAC-3′ and 5′-TTTTGAAGAGCACAGAACACCT-3′; *TMPRSS2*: 5′-TGGTCCTGGATGATAAAAAAAGTTT-3′ and 5′-GACATACGCCCCACAACAGA -3′.

Mouse xenograft studies

Male NSG mice, 6 to 8 weeks of age were obtained from the Cleveland Clinic Biological Resources Unit facility. All mouse studies were conducted under a protocol approved by the Cleveland Clinic Institutional Animal Care and Use Committee. Sample size was determined based on our prior studies of steroidogenesis inhibition in xenograft models of CRPC[3,13]. Criteria for progression were determined based on similar criteria that are utilized for clinical progression. Mice were surgically orchiectomized and implanted with a 5 mg 90-day sustained-release DHEA pellet (Innovative Research of America) to mimic CRPC in the context of human adrenal physiology. Two days later, 10^7 VCaP or C4-2 cells were injected subcutaneously with matrigel. Once tumors reached 300 mm^3 (length × width × height × 0.52), mice were arbitrarily (but not strictly randomized) assigned to vehicle (n=9 or 10 mice for VCaP and C4-2 respectively), Abi acetate (n=10 mice for both cell lines), D4A (n=10 mice for both cell lines) or enzalutamide (n=11 for C4-2) treatment groups. Abi acetate and D4A (0.5 mmol/kg/d in 0.1 mL 5% benzyl alcohol and 95% safflower oil solution) were administered via 5 mL/kg intraperitoneal injection every day for up to 15 days. Control groups were administered 0.1 mL 5% benzyl alcohol and 95% safflower oil solution via intraperitoneal injection every day. Mice in enzalutamide group were fed with enzalutamide in chow every day (10mg/Kg/day)[25]. Treatment was not blinded to the investigator. Tumor volume was measured daily, and time to increase in tumor volume by 20% was determined. Mice were sacrificed at treatment day 15 or when the tumor size was 2-fold greater than baseline. The significance of the difference between treatment groups was assessed by Kaplan-Meier survival analysis using a log-rank test in SigmaStat 3.5. Two-tailed student's t-test was used to determine significance in Extended Data Fig. 6.

Enzyme assays

To test D4A as an inhibitor of 3βHSD, enzyme assays were performed as described previously[10]. Briefly, incubations were prepared with recombinant human 3βHSD1 or 3βHSD2 (in yeast microsomes, 45 or 2.5 μg protein per incubation, respectively), [^{3}H]-pregnenolone (100,000 cpm, 1–20 μmol/L), and D4A (5–20 μmol/L) or ethanol vehicle in 0.5 mL of potassium phosphate buffer (pH 7.4). After a pre-incubation at 37°C for 1 to 3 min, NAD^+ (1 mmol/L) was added, and the incubation was conducted at 37°C for 20 min. The reaction was stopped by addition of 1 mL ethyl acetate:isooctane (1:1), and the steroids

were then extracted into the organic phase and dried. The steroids in the dried extracts were resolved by HPLC and quantitated by in-line scintillation counting.

AR competition assay

Cells were cultured in serum-free medium for 48 h and then treated with [^{3}H]-R1881 and the indicated concentrations of D4A, Abi, enzalutamide, R1881 or bicalutamide for 30 min. Cells were washed with 1X PBS 4 times and 0.9% NaCl solution twice before lysis with RIPA buffer. Intracellular radioactivity was measured with a Beckman Coulter LS60001C liquid scintillation counter and normalized to the protein concentration as detected with a Wallac Victor2 1420 Multilabel counter (Perkin Elmer).

Cell proliferation assay

LNCaP cells (0.1 million/mL) were seeded in 96-well plates and cultured in phenol red free RPMI-1640 mediums plus 10% charcoal stripped FBS with androgens and/or drugs. Medium was changed every other day. After 2, 4 or 6 days, cells were collected and lysed after treatment. Growth was then determined based on DNA content as detected by Hoechst stain and a Wallac Victor2 1420 Multilabel counter (Perkin Elmer). Two-tailed student's t-test was used to determine significance.

Mass spectrometry

Patient serum collection and drug extraction—Twelve patients with CRPC undergoing treatment with Abi acetate were consented under an Institutional Review Board – approved protocol (Case 7813). Blood was collected using Vacutainer Plus serum blood collection tubes (#BD367814, Becton Dickenson, Franklin Lakes, NJ). Blood was collected between 2 and 14 hours after the 1000mg daily dose of Abi acetate was administered. Blood was allowed to clot and tubes were centrifuged at 2500 RPM for 10 minutes. Serum aliquots were frozen at −80°C until processing. Drug metabolites and internal standard (d_4-cortisol, CDN isotopes Pointe-Claire, Quebec Canada) were extracted from 200 μL of patient serum with methyl tert-butyl ether (Sigma Aldrich, St. Louis, MO), evaporated under a stream of nitrogen gas and reconstituted in methanol prior to mass spectrometry analysis.

Mouse serum collection, derivatization and extraction—At the completion of the mouse xenograft study, mouse serum was collected for steroid analysis. 20 μl of serum and internal standard (d_8-deoxycorticosterone) was derivatized with hydroxylamine (Sigma Aldrich, St. Louis, MO)[26]. Steroids were extracted with methyl tert-butyl ether (Sigma Aldrich, St. Louis, MO), evaporated under a stream of nitrogen gas and reconstituted in methanol:water (50:50) prior to mass spectrometry analysis.

Stable isotope dilution liquid chromatography mass spectrometry analysis

Mouse serum analysis—Samples were analyzed on a Thermo TSQ Quantiva-Prelude SPLC system (Thermo Scientific, Waltham, MA) with Aria MX 2.1 and Tracefinder 3.2.368.22 software for instrument controls and quantitation. Analyte separation was achieved with a Accucore 50 × 3mm, 2.6μm C18 column (Thermo Scientific, Waltham, MA) using a mobile phase of LCMS grade methanol and water (Thermo Scientific,

Waltham, MA), a gradient of 25–100% methanol, and a flow rate of 0.6 ml/min. Steroids were ionized by electrospray ionization and in positive ion mode. Multiple reaction monitoring was used to follow mass transitions for the oximes of deoxycorticosterone (m/z: 361.2/124.1) and d_8-deoxycorticosterone (m/z: 369.4/128.1) (Steraloids Newport, RI). Concentrations were determined using stable isotope dilution analysis.

Patient serum analysis—Blood was obtained from prostate cancer patients with consent under a protocol approved by the Cleveland Clinic Institutional Review Board. Samples were analyzed on a ultra high-performance liquid chromatography station (Shimadzu, Kyoto, Japan) with a DGU-20A3R degasser, 2 LC-30AD pumps, a SIL-30AC autosampler, a CTO-10A column oven and a CBM-20A system controller in tandem with a QTRAP 5500 mass spectrometer (AB Sciex, Framingham, MA). The mobile phase consisted of LC-MS grade (Fisher) methanol: acetonitrile: water (44:36:20). Separation of drug metabolites was achieved using a Zorbax Eclipse plus 150 × 2.1 mm, 3.5μm C18 column (Agilent, Santa Clara, CA) at a flow rate of 0.2 ml/min. Drug metabolites were ionized using electrospray ionization in positive ion mode. Multiple reaction monitoring was used to follow mass transitions for D4A (m/z: 348.2/156.3), abiraterone (m/z: 350.3/156.1), and d_4-cortisol (m/z: 367.1/121.1). Standard curves were generated using human serum spiked with known concentrations of each metabolite to enable determination of unknown concentrations in patient samples.

Extended Data

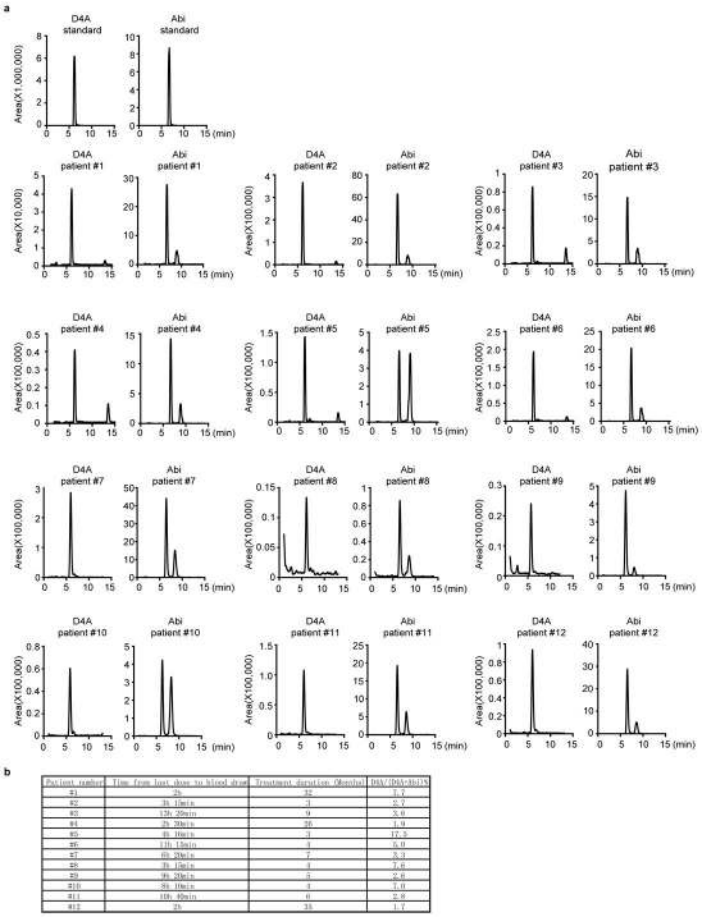

Patient number	Time from last dose to blood draw	Treatment duration (Months)	D4A/(D4A+Abi)(%)
#1	2h	32	1.7
#2	3h 18min	3	5.7
#3	13h 25min	9	3.0
#4	2h 30min	20	1.9
#5	6h 16min	1	12.3
#6	11h 13min	3	5.0
#7	6h 23min	7	3.3
#8	3h 18min	3	7.8
#9	9h 23min	5	2.6
#10	9h 10min	3	5.0
#11	10h 40min	6	2.9
#12	2h	35	1.7

Extended Data Figure 1.

D4A is detectable in prostate cancer patients treated with Abi acetate. a, Mass spectrometry tracings of Abi and D4A in the serum of 12 patients treated with Abi acetate. Blood was drawn between 2 and 14 hours after the administration of the 1000 mg daily dose. b, Duration of Abi acetate therapy and time from last dose to blood draw for individual patients.

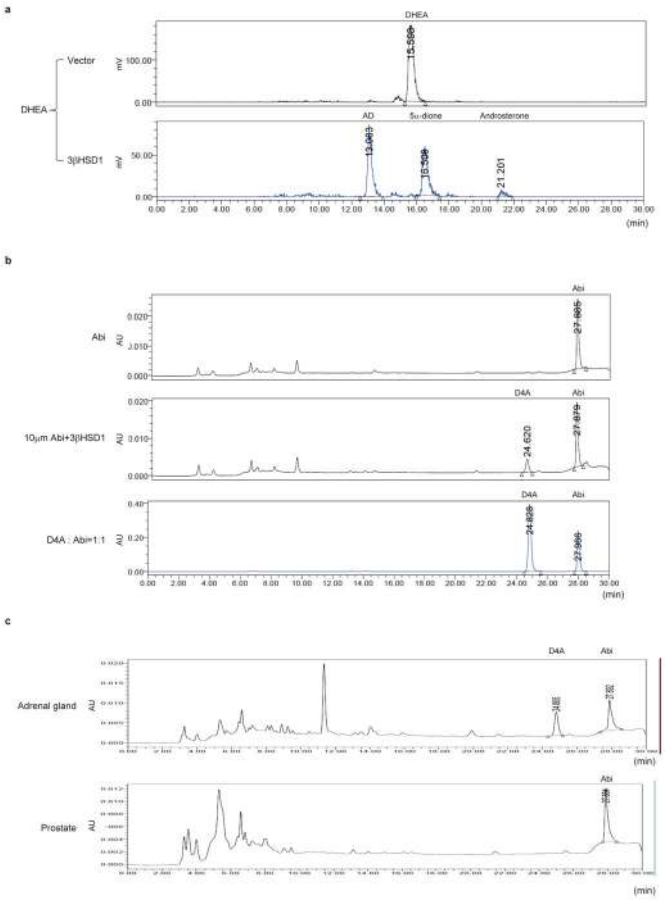

Extended Data Figure 2.

3βHSD converts Abi to D4A. a, 3βHSD1 expression permits catalysis of DHEA to AD. LAPC4 cells were transfected with 3βHSD1 or vector and treated with [^{3}H]-DHEA. Medium was collected 24h later and androgens were separated and quantified by HPLC. b, 3βHSD1 expression allows conversion of Abi to D4A. LAPC4 cells were transfected with 3βHSD1 or vector and then treated with Abi. Medium was collected after 24h and D4A and Abi were separated by HPLC. c, 3βHSD enzymatic activity present in the mouse adrenal but not prostate converts Abi to D4A. Mouse adrenals and prostate were harvested and minced before culturing in the presence of media containing Abi. Medium was collected after 24h for separation and quantitation of D4A and Abi by HPLC.

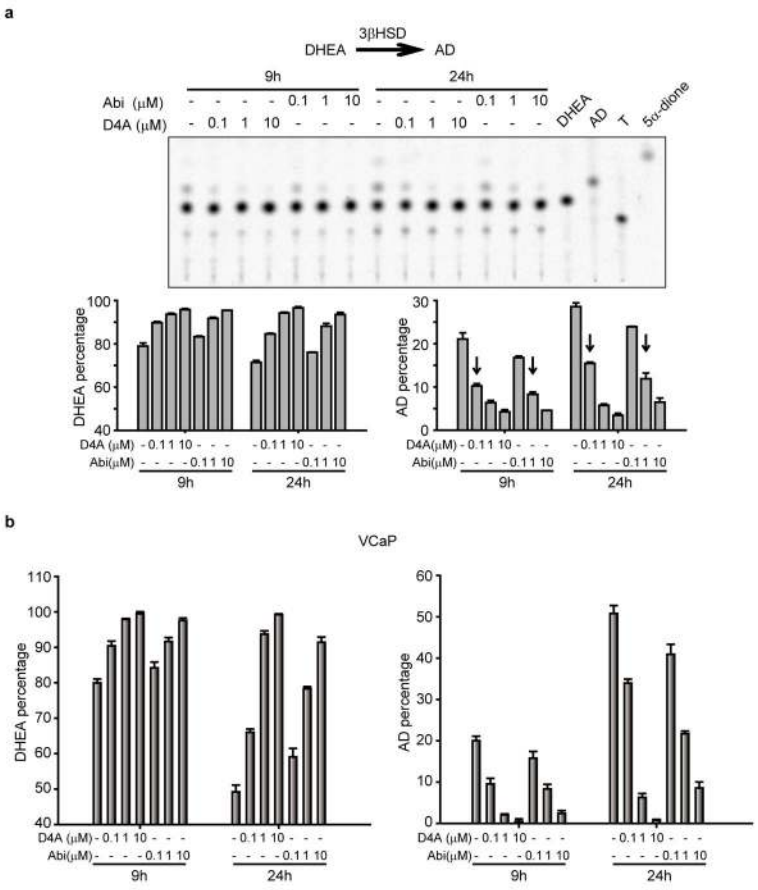

Extended Data Figure 3.

D4A inhibits 3βHSD1 activity. a, D4A inhibits 3βHSD1 activity in LNCaP. Cells were treated with [^{3}H]-DHEA (DHEA: 100nM; [^{3}H]-DHEA, 1,000,000 cpm/well) with 0.1, 1 or 10 μM D4A and Abi, for 9 and 24 hours. DHEA and AD were separated and quantified by TLC. ImageJ was used to quantify steroids. For ease of comparison, arrows denote AD percentage for 0.1 μM D4A and 1 μM Abi treatment groups. b, VCaP cells were treated with [^{3}H]-DHEA and the indicated concentrations of D4A and Abi. The percentages of DHEA and AD were determined by HPLC. Experiments were performed with biological replicates (n = 3) and results are shown as mean ± s.d.

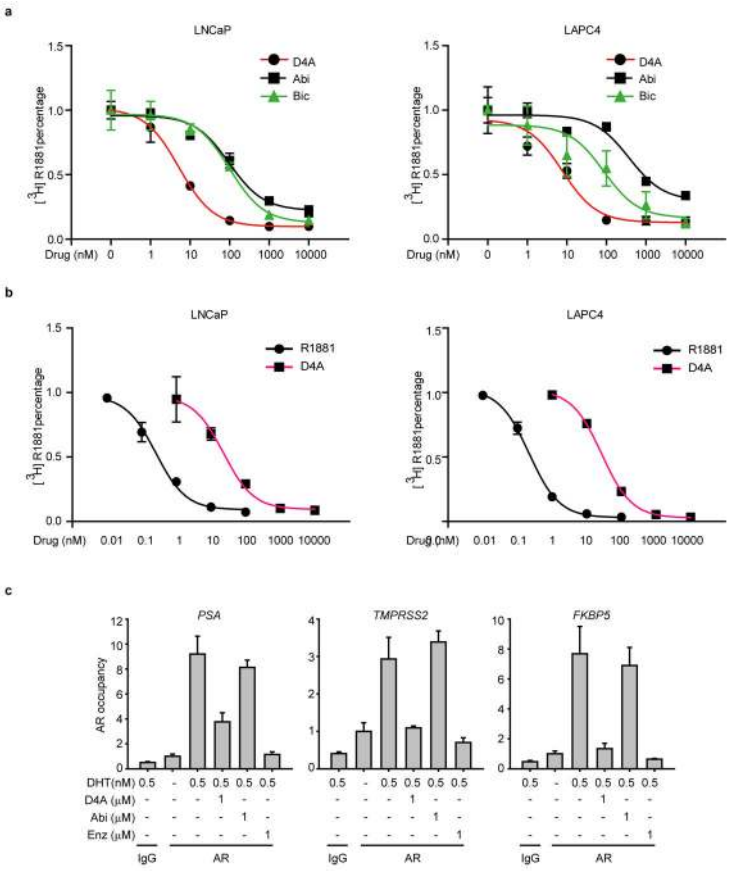

Extended Data Figure 4.

D4A has a higher affinity for both mutant type AR (LNCaP cells) and wild-type AR (LAPC4 cells) than abiraterone (Abi) and bicalutamide (Bic) and inhibits AR chromatin occupancy better than Abi. a, Competition plots for D4A, Abi and Bic. b, Competition plots for unlabeled R1881 and D4A. Displacement of [^{3}H]-R1881 is described in the Methods section. Experiments were performed with biological replicates (n = 3) and results are shown as mean ± s.d. c, D4A inhibition of AR chromatin occupancy is superior to Abi. LNCaP cells were treated with the indicated concentrations of DHT, D4A, Abi and enzalutamide (Enz) for 3h. AR chromatin occupancy for *PSA*, *TMPRSS2* and *FKBP5* was detected with ChIP. Experiments were performed with technical replicates (n = 3) and results are shown as mean ± s.d. All experiments were repeatedly independently at least 3 times.

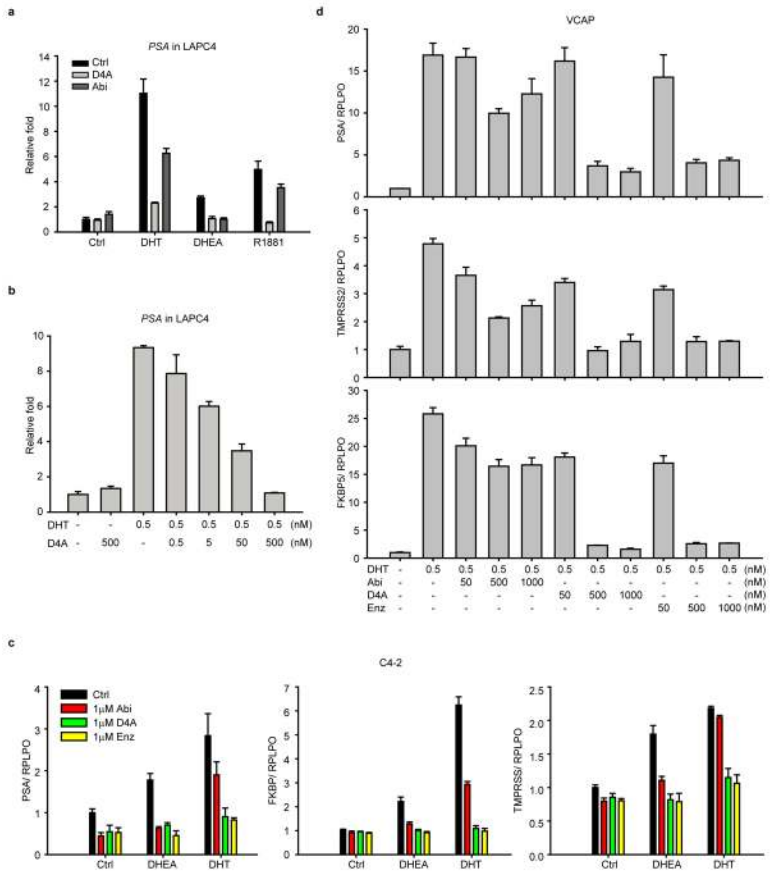

Extended Data Figure 5.

D4A inhibits expression of androgen-responsive genes. a, D4A inhibits *PSA* expression in LAPC4 cells. Cells were treated with DHT (0.5 nM), DHEA (40 nM) or R1881 (0.1 nM) with or without Abi or D4A (1 μM) for 24h. b, D4A inhibits *PSA* expression in LAPC4 in a dose-dependent manner. c, D4A inhibits AR target gene expression in C4-2 cells. Cells were treated with vehicle control (Ctrl), DHT (0.5 nM) or DHEA (40 nM) with or without Abi (1 μM), D4A (1 μM) or Enz (1 μM) for 24h. d, D4A is comparable to Enz in inhibiting DHT-induced target gene expression in VCaP cells. Gene expression was assessed in triplicate and detected by qPCR and normalized to *RPLP0*. Experiments were performed with technical replicates (n = 3) and results are shown as mean ± s.d. All experiments were repeatedly independently at least 3 times.

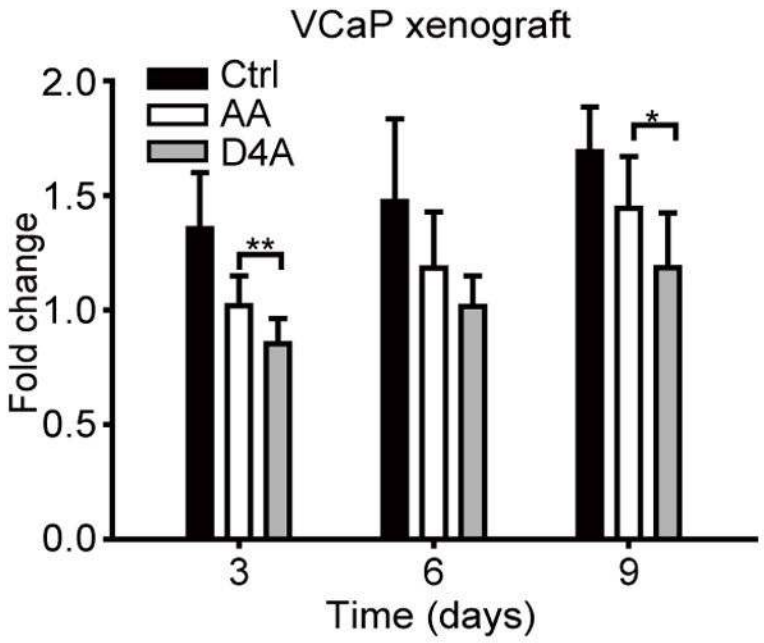

Extended Data Figure 6.

D4A impedes VCaP xenograft growth. * and ** denote *P* values < 0.05 and 0.01, respectively, for the difference between D4A (n = 10 mice) and AA (n = 10 mice) treatment groups. N = 9 mice for the control group.

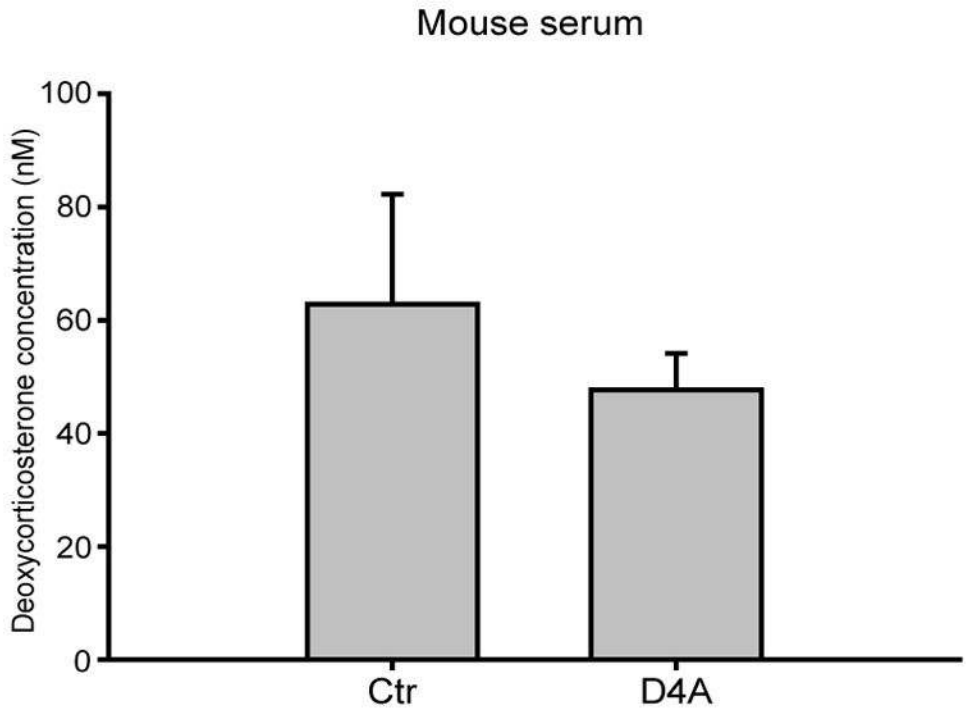

Extended Data Figure 7.

D4A does not increase deoxycorticosterone concentrations. Serum of mice undergoing long term treatment with D4A was collected and deoxycorticosterone concentrations were determined by LC-MS. Compared to control mice injected with vehicle, D4A does not increase deoxycorticosterone concentrations. For both D4A and control groups, n = 9 biological replicates (mice).

Acknowledgments

This work has been supported in part by funding from a Howard Hughes Physician-Scientist Early Career Award (to N.S.), by the Prostate Cancer Foundation (to N.S.), by an American Cancer Society Research Scholar Award (12-038-01-CCE; to N.S.), grants from the U.S. Army Medical Research and Materiel Command (PC080193 to N.S. and PC121382 to Z.L.), and additional grants from the National Cancer Institute (R01CA168899, R01CA172382, and R01CA190289; to N.S.).

References

1. Titus MA, Schell MJ, Lih FB, Tomer KB, Mohler JL. Testosterone and dihydrotestosterone tissue levels in recurrent prostate cancer. Clin Cancer Res: an official journal of the American Association for Cancer Research. 2005; 11:4653–4657. 11/13/4653 [pii]. 10.1158/1078-0432.CCR-05-0525
2. Montgomery RB, et al. Maintenance of intratumoral androgens in metastatic prostate cancer: a mechanism for castration-resistant tumor growth. Cancer Res. 2008; 68:4447–4454. 68/11/4447 [pii]. 10.1158/0008-5472.CAN-08-0249 [PubMed: 18519708]
3. Chang KH, et al. A gain-of-function mutation in DHT synthesis in castration-resistant prostate cancer. Cell. 2013; 154:1074–1084.10.1016/j.cell.2013.07.029 [PubMed: 23993097]
4. Knudsen KE, Penning TM. Partners in crime: deregulation of AR activity and androgen synthesis in prostate cancer. Trends Endocrinol Metab. 2010; 21:315–324. S1043–2760(10)00004-4 [pii]. 10.1016/j.tem.2010.01.002 [PubMed: 20138542]
5. Chang KH, Sharifi N. Prostate cancer-from steroid transformations to clinical translation. Nat Rev Urol. 2012; 9:721–724. nrurol.2012.175 [pii]. 10.1038/nrurol.2012.175 [PubMed: 23027067]
6. de Bono JS, et al. Abiraterone and increased survival in metastatic prostate cancer. N Engl J Med. 2011; 364:1995–2005.10.1056/NEJMoa1014618 [PubMed: 21612468]
7. Ryan CJ, et al. Abiraterone in Metastatic Prostate Cancer without Previous Chemotherapy. N Engl J Med. 201210.1056/NEJMoa1209096
8. Scher HI, et al. Increased survival with enzalutamide in prostate cancer after chemotherapy. N Engl J Med. 2012; 367:1187–1197.10.1056/NEJMoa1207506 [PubMed: 22894553]
9. Beer TM, et al. Enzalutamide in metastatic prostate cancer before chemotherapy. N Engl J Med. 2014; 371:424–433.10.1056/NEJMoa1405095 [PubMed: 24881730]
10. Li R, et al. Abiraterone inhibits 3beta-hydroxysteroid dehydrogenase: a rationale for increasing drug exposure in castration-resistant prostate cancer. Clin Cancer Res. 2012; 18:3571–3579.10.1158/1078-0432.ccr-12-0908 [PubMed: 22753664]
11. Ferraldeschi R, Sharifi N, Auchus RJ, Attard G. Molecular Pathways: Inhibiting Steroid Biosynthesis in Prostate Cancer. Clin Cancer Res. 2013; 19:3353–3359.10.1158/1078-0432.Ccr-12-0931 [PubMed: 23470964]
12. Garrido M, et al. A-ring modified steroidal azoles retaining similar potent and slowly reversible CYP17A1 inhibition as abiraterone. J Steroid Biochem Mol Biol. 2014; 143:1–10.10.1016/j.jsbmb.2014.01.013 [PubMed: 24508512]
13. Chang KH, et al. Dihydrotestosterone synthesis bypasses testosterone to drive castration-resistant prostate cancer. Proceedings of the National Academy of Sciences of the United States of America. 2011; 108:13728–13733. 1107898108 [pii]. 10.1073/pnas.1107898108 [PubMed: 21795608]
14. Richards J, et al. Interactions of Abiraterone, Eplerenone, and Prednisolone with Wild-type and Mutant Androgen Receptor: A Rationale for Increasing Abiraterone Exposure or Combining with MDV3100. Cancer Res. 2012; 72:2176–2182. 0008-5472.CAN-11-3980 [pii]. 10.1158/0008-5472.CAN-11-3980 [PubMed: 22411952]

15. Hodgson MC, et al. The androgen receptor recruits nuclear receptor CoRepressor (N-CoR) in the presence of mifepristone via its N and C termini revealing a novel molecular mechanism for androgen receptor antagonists. J Biol Chem. 2005; 280:6511–6519.10.1074/jbc.M408972200 [PubMed: 15598662]
16. Attard G, et al. Phase I clinical trial of a selective inhibitor of CYP17, abiraterone acetate, confirms that castration-resistant prostate cancer commonly remains hormone driven. J Clin Oncol. 2008; 26:4563–4571. JCO.2007.15.9749 [pii]. 10.1200/JCO.2007.15.9749 [PubMed: 18645193]
17. Carreira S, et al. Tumor clone dynamics in lethal prostate cancer. Sci Transl Med. 2014; 6:254ra125.10.1126/scitranslmed.3009448
18. Balk, S. AACR-Prostate Cancer Foundation Conference on Advances in Prostate Cancer Research;
19. Attard G, et al. Clinical and biochemical consequences of CYP17A1 inhibition with abiraterone given with and without exogenous glucocorticoids in castrate men with advanced prostate cancer. J Clin Endocrinol Metab. 2012; 97:507–516.10.1210/jc.2011-2189 [PubMed: 22170708]
20. Efstathiou E, et al. Enzalutamide (ENZA) in combination with abiraterone acetate (AA) in bone metastatic castration resistant prostate cancer (mCRPC). ASCO Meeting Abstracts. 2014; 32:5000.
21. Dreicer R, Jones R, Oudard S, Efstathiou E, Saad F, de Wit R, De Bono J, et al. A phase 3, randomized, double-blind, multicenter trial comparing orteronel (TAK-700) plus prednisone with placebo plus prednisone in patients with metastatic castration-resistant prostate cancer that has progressed during or following docetaxel-based therapy: ELM-PC 5. J Clin Oncol. (In press).
22. Papari-Zareei M, Brandmaier A, Auchus RJ. Arginine 276 controls the directional preference of AKR1C9 (rat liver 3alpha-hydroxysteroid dehydrogenase) in human embryonic kidney 293 cells. Endocrinology. 2006; 147:1591–1597.10.1210/en.2005-1141 [PubMed: 16357042]
23. Li Z, Nie F, Wang S, Li L. Histone H4 Lys 20 monomethylation by histone methylase SET8 mediates Wnt target gene activation. Proc Natl Acad Sci U S A. 2011; 108:3116–3123.10.1073/pnas.1009353108 [PubMed: 21282610]
24. Evaul K, Li R, Papari-Zareei M, Auchus RJ, Sharifi N. 3β-hydroxysteroid dehydrogenase is a possible pharmacological target in the treatment of castration-resistant prostate cancer. Endocrinology. 2010; 151:3514–3520. en.2010-0138 [pii]. 10.1210/en.2010-0138 [PubMed: 20534728]
25. Tran C, et al. Development of a second-generation antiandrogen for treatment of advanced prostate cancer. Science. 2009; 324:787–790. 1168175 [pii]. 10.1126/science.1168175 [PubMed: 19359544]
26. Kushnir MM, et al. Liquid chromatography-tandem mass spectrometry assay for androstenedione, dehydroepiandrosterone, and testosterone with pediatric and adult reference intervals. Clinical chemistry. 2010; 56:1138–1147.10.1373/clinchem.2010.143222 [PubMed: 20489135]

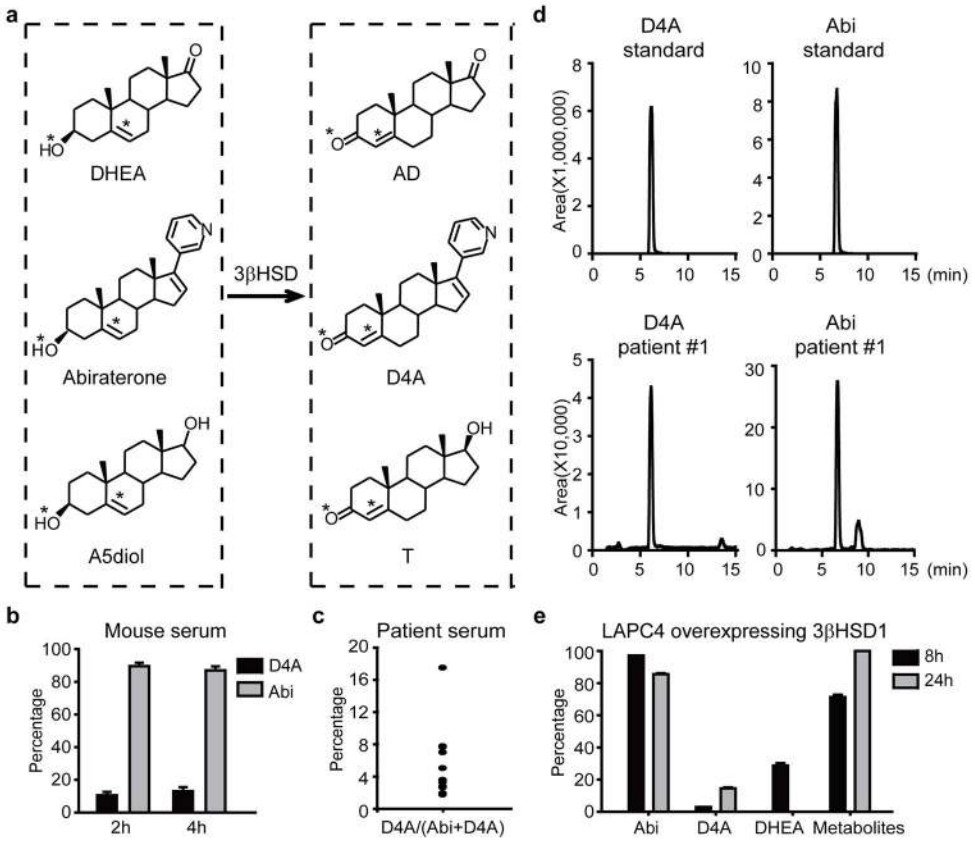

Figure 1.

Structural consequences of the conversion from Abi to D4A that occurs in both mice, and patients, and requires 3βHSD. a, Schematic of Abi conversion to D4A. * double bond and C3-position for substrates and products of 3βHSD. b, Abi is converted to D4A *in vivo*. Abi acetate was injected i.p. in 5 mice. Blood was collected 2h and 4h after injection. Serum concentrations of Abi and D4A were quantified by mass spectrometry and are represented as the percentage of the sum total of Abi + D4A. c, D4A is detectable in all patients (n = 12) with CRPC treated with Abi acetate. d, Representative mass spectrometry tracing of D4A and Abi from the serum of a patient treated with Abi acetate. e, 3βHSD1 is capable of converting Abi to D4A. LAPC4 cells overexpressing 3βHSD1 were treated with 10μM Abi (or [^{3}H]-DHEA) for 24h. Abi, D4A (as a percentage of Abi + D4A), [^{3}H]-DHEA and [^{3}H]-DHEA metabolites (labeled metabolites), were separated by HPLC. Results are shown as mean (n = 3) ± s.d. with biological replicates. The experiment was repeated independently at least 3 times.

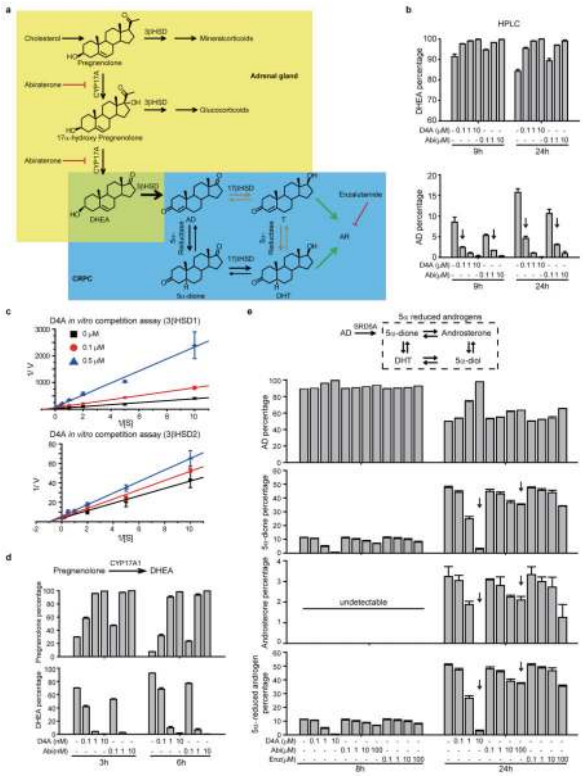

Figure 2.

D4A inhibits 3βHSD, CYP17A, and 5α-reductase enzymatic activity in the androgen pathway. a, Schematic of the steroidogenesis pathway from adrenal precursors to DHT and AR stimulation in CRPC. b, D4A inhibits 3βHSD1 activity in LNCaP. Cells were treated with [^{3}H]-DHEA with 0.1, 1 or 10 μM D4A and Abi, for 9 and 24 hours. DHEA and AD were quantified by HPLC. Arrows denote AD percentage for 0.1 μM D4A and 1 μM Abi treatment groups. c, Lineweaver-Burk plots of pregnenolone metabolism and D4A inhibition of human 3βHSD1 and 3βHSD2 activity. D4A shows mixed competitive-noncompetitive inhibition for 3βHSD1 and noncompetitive inhibition for 3βHSD2. d, CYP17A1 inhibition with D4A is comparable to Abi. 293 cells stably expressing CYP17A1 were treated with 0.1, 1 or 10 nM D4A, or Abi, together with [^{3}H]-pregnenolone for 3 and 6 hours. Pregnenolone and DHEA were separated and quantified by HPLC. e, D4A but not Abi or enzalutamide inhibits 5α-reductase activity. LAPC4 cells were treated with [^{3}H]-AD and the indicated drug concentrations. Steroids were quantified by HPLC. Arrows denote 5α-reduced androgen percentage for 10 μM D4A and 100 μM Abi treatment groups. All experiments performed with biological replicates (n = 3) and repeated independently three times. All results are shown as mean ± s.d..

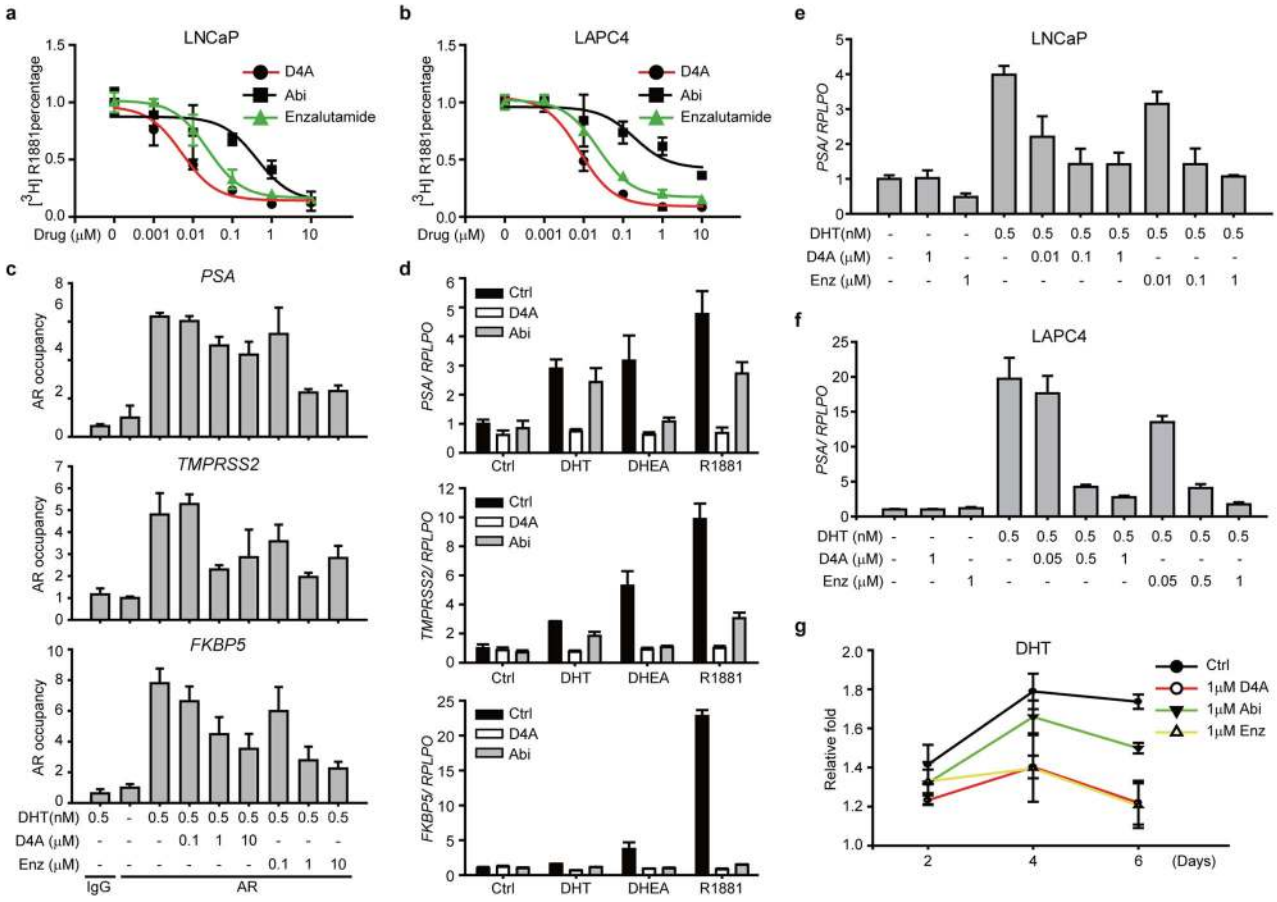

Figure 3.

D4A binds to AR, inhibits AR chromatin occupancy, expression of AR-responsive genes and cell growth. a and b, D4A potently binds to both mutant and wild-type AR. D4A, Abi and enzalutamide (Enz) (0.001–10 μM) were used to compete with 0.1nM [^{3}H]-R1881 for mutated AR (LNCaP) or wild type AR (LAPC4). Intracellular radioactivity was normalized to protein concentration. c, Dose-dependence of D4A versus Enz for inhibition of AR chromatin occupancy. LNCaP cells were treated with the indicated concentrations of DHT, D4A, and Enz for 3h. AR chromatin occupancy for *PSA*, *TMPRSS2* and *FKBP5* was detected with ChIP. AR ChIP is normalized to untreated control for each gene. d, D4A inhibits *PSA*, *FKBP5* and *TMPRSS2* expression. LNCaP cells were treated with DHT (0.5 nM), DHEA (40 nM) or R1881 (0.1 nM) with or without Abi or D4A (1μM) for 24h. Gene expression was detected by qPCR and normalized to *RPLP0*. e and f, D4A inhibition of DHT induced *PSA* expression is comparable to Enz in LNCaP and LAPC4. g, D4A inhibits DHT (0.5 nM) induced cell growth in LNCaP. Cells were quantified at the indicated time points by assaying DNA content after 2, 4 and 6 days of treatment. Experiments in a, b and g were performed with biological replicates; c–f were performed with technical replicates. All experiments were repeated independently three times. All results are shown as mean (n = 5 for panel g; n = 3 for all other experiments) ± s.d.

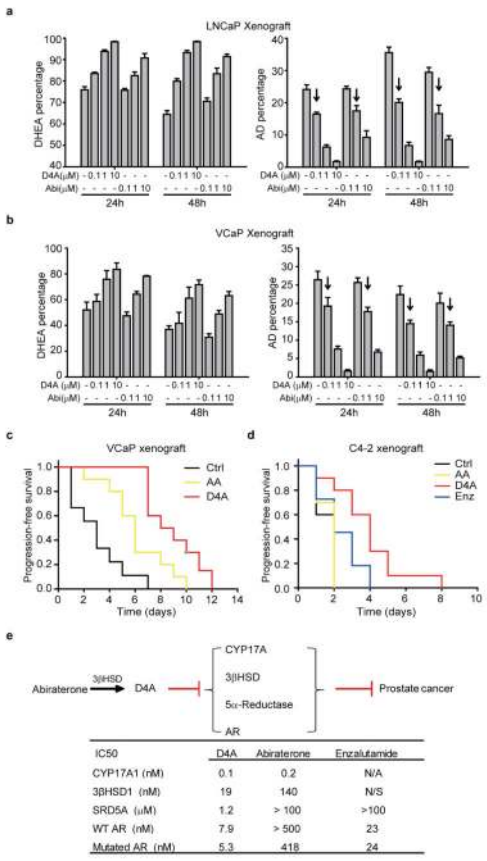

IC50	D4A	Abiraterone	Enzalutamide
CYP17A1 (nM)	0.1	0.2	N/A
3βHSD1 (nM)	19	140	N/S
SRD5A (μM)	1.2	> 100	>100
WT AR (nM)	7.9	> 500	23
Mutated AR (nM)	5.3	418	24

Figure 4.

D4A inhibits xenograft steroidogenesis and growth. a and b, D4A inhibits steroidogenesis in LNCaP and VCaP xenografts. Xenografts were grown subcutaneously in NSG mice. Xenografts reaching ~1000 mm^3 were minced and treated with [^{3}H]-DHEA, plus Abi or D4A (0.1, 1 and 10μM). DHEA and AD were separated and quantified by HPLC. Experiments were performed with biological replicates (n = 3 xenograft tissues) and results are shown as mean ± s.d. Arrows denote AD percentage for 0.1 μM D4A and 1 μM Abi treatment groups. c, D4A is more potent than Abi for blocking VCaP xenograft progression. Time to xenograft progression (> 20% increase in tumor volume) is shown for vehicle (Ctrl; n = 9 mice), Abi acetate (AA; n = 10) and D4A (n = 10) treatment groups. All 3 treatment groups differ significantly from one another: Ctrl vs AA, $P = 0.02$; Ctrl vs D4A, $P < 0.001$; AA vs D4A, $P = 0.01$. d, D4A (n = 10) is more potent than AA (n = 10) and Enz (n = 11) for blocking C4-2 xenograft progression: Ctrl vs D4A, $P < 0.001$; AA vs D4A, $P = 0.01$; Enz vs D4A, $P = 0.02$. e, Schematic of D4A activities and IC_{50} in the androgen pathway and comparisons with Abi and Enz.